AIAA JOURNAL
Vol. 41, No. 8, August 2003

Surface Properties During Primary Breakup of Turbulent Liquid Jets in Still Air

K. A. Sallam* and G. M. Faeth†
University of Michigan, Ann Arbor, Michigan 48109-2140

The formation of ligaments and drops at the liquid surface during primary breakup of turbulent liquid jets in still air, that is, during turbulent primary breakup, was studied experimentally using pulsed shadowgraphy and holography. Experimental conditions included round and plane (the latter actually being annular with a large aspect ratio) turbulent liquid jets in still air at normal temperature and pressure for noncavitating water and ethanol flows, long length/hydraulic-diameter (greater than 40:1) injector passages to provide fully developed turbulent pipe flow at the jet exit, jet exit Reynolds numbers of 6×10^3–4.24×10^5, jet exit Weber numbers of 200–300,000, and liquid/gas density ratios of 690 and 860 at conditions where direct effects of liquid viscosity were small (for example, jet exit Ohnesorge numbers were smaller than 0.0053). Measured properties included liquid surface velocities, conditions at the onset of ligament and drop formation, ligament and drop sizes along the surface, and ligament and drop velocities along the surface and rates of drop formation along the surface. Simplified phenomenological theories were used to help interpret and correlate the measurements.

Nomenclature

A_ℓ	=	ligament projected area
b	=	annulus width
$C_{\ell i}$	=	coefficient of the $d_{\ell i}$ correlation
$C_{\ell x}$	=	coefficient of the $d_\ell(x)$ correlation
C_s	=	coefficient of the Sauter mean diameter at onset of drop formation (SMD_i) correlation
C_{sx}	=	coefficient of the SMD(x) correlation
C_{xr}	=	coefficient of the $(x_i - x_{\ell i})/(u_0 t_{ri})$ correlation
d	=	round jet exit diameter
d_h	=	jet exit hydraulic diameter
d_ℓ	=	ligament effective diameter; Eq. (1)
$d_{\ell i}$	=	d_ℓ at onset of ligament formation
L_a	=	aerodynamic ligament breakup length
L_c	=	mean ligament breakup length
L_ℓ	=	ligament length at breakup
$\dot{m}''_f$	=	mass flux of drops relative to surface
Oh_{fd}	=	jet exit Ohnesorge number, $\mu_f/(\rho_f d_h \sigma)^{1/2}$
Re_{fd}	=	jet exit Reynolds number, $\rho_f u_0 d_h/\mu_f$
$Re_{f\ell}$	=	ligament Reynolds number, $\rho_f u_\ell d_\ell/\mu_f$
t_a	=	aerodynamic ligament breakup time
$t_{\ell i}$	=	ligament breakup time at onset of ligament formation
t_r	=	Rayleigh breakup time of a ligament of diameter d_ℓ
t_{ri}	=	Rayleigh breakup time at onset of drop formation
u_ℓ	=	velocity along ligament axis
$\bar{u}_s$	=	mean streamwise surface velocity
u_0	=	average streamwise velocity at jet exit
$\tilde{u}$	=	mass averaged streamwise drop velocity
$v_{\ell i}$	=	velocity of characteristic eddy at onset of ligament formation
$\tilde{v}_r$	=	mass average cross stream drop velocity relative to surface
$\bar{v}'_0$	=	average rms cross stream velocity fluctuation at jet exit
v_λ	=	characteristic velocity of eddy of size λ
$v_{\lambda i}$	=	characteristic velocity of eddy of size λ_i
We_{fd}	=	jet exit Weber number based on d_h, $\rho_f u_0^2 d_h/\sigma$
$We_{f\ell}$	=	Weber number based on ligament properties, $\rho_f u_\ell^2 d_\ell/\sigma$
$We_{f\Lambda}$	=	jet exit Weber number based on Λ, $\rho_f \bar{u}_0^2 \Lambda/\sigma$
x	=	streamwise length from jet exit
x_i	=	streamwise length to initiate drop formation
$x_{\ell i}$	=	streamwise length to initiate ligament formation
δ	=	initial amplitude of a disturbance
ε	=	surface efficiency factor; Eq. (37)
Λ	=	cross stream integral length scale, $d_h/8$
λ	=	characteristic eddy size
λ_i	=	characteristic eddy size at onset of ligament formation
μ_f	=	molecular viscosity of liquid
ν_g	=	kinematic viscosity of gas
ρ_f	=	liquid density
ρ_g	=	gas density
σ	=	surface tension
ϕ	=	ligament angle

Introduction

DROP formation along the surface of turbulent liquids in either still or slow moving gases, called turbulent primary breakup, is the mechanism of spray formation during a variety of industrial and natural processes, for example, spray atomization, chutes, spillways, plunge pools, hydraulic jumps, ship bow waves, ship wakes, breaking waves, whitecaps, and waterfalls, among others. The mechanism of turbulent primary breakup was identified during the early flow visualization studies of De Juhasz et al.[1] and Lee and Spenser.[2,3] Subsequent studies due to Schweitzer,[4] Grant and Middleman,[5] Phinney,[6] and McCarthy and Malloy[7] confirmed that liquid turbulence properties at the jet exit affected jet stability, the onset of drop formation (the onset of breakup) and spray quality after breakup. Finally, Hoyt and Taylor[8,9] showed that drop formation due to turbulent primary breakup was associated with the formation of ligaments along the liquid surface and that aerodynamic effects were generally of secondary importance for turbulent primary breakup at the surface of turbulent liquids in still or slowly moving air at normal temperature and pressure (NTP).

Subsequent studies of turbulent primary breakup were undertaken in this laboratory as follows: Studies at the surface of turbulent round liquid jets in still gases are due to Ruff et al.,[10–12] Tseng et al.,[13] Wu et al.,[14] Wu and Faeth,[15] Wu et al.,[16] Wu and Faeth,[17] and Sallam et al.[18] Studies at the surface of turbulent annular (nearly plane) wall jets in still gases are due to Dai et al.[19,20] Studies at the surface of

Received 7 May 2002; revision received 25 November 2002; accepted for publication 4 March 2003.

*Postdoctoral Research Fellow, Department of Aerospace Engineering, 1320 Beal Avenue.

†A. B. Modine Professor, Department of Aerospace Engineering, 1320 Beal Avenue; gmfaeth@umich.edu. Fellow AIAA.

turbulent annular (nearly plane) freejets are due to Sallam et al.[21] During these studies, pulsed shadowgraphy and holography were used to measure the properties of turbulent primary breakup due to the capabilities of these techniques to resolve the properties of irregularly shaped drops within the dense sprays, caused by turbulent primary breakup along the surface of turbulent liquids in still gases, as follows: Aerodynamic effects were small for liquid/gas density ratios greater than 500 (typical of injection of liquids into air and other light gases at NTP), except far from the jet exit where turbulent primary breakup and secondary breakup occur at comparable times and tend to merge.[15] Drop size distributions after turbulent primary breakup satisfied the universal root normal distribution of Simmons[22] and are completely defined by the Sauter mean diameter (SMD) (i.e., the diameter of a drop having the same surface-area/volume ratio as the spray as a whole). Drop velocities after turbulent primary breakup were independent of drop size and were simply related to mean and rms fluctuating velocities of the liquid at the jet exit. The SMD of drops after turbulent primary breakup progressively increase with increasing distance along the liquid surface and could be correlated based on simplified phenomenological analysis. The use of hydraulic diameter concepts yielded correlations of turbulent primary breakup properties that were identical for round and annular (nearly plane) turbulent freejets. In addition, some preliminary information was obtained about the rate of drop formation along the liquid surface due to turbulent primary breakup of round free turbulent jets in still air.

The objective of the present experimental investigation was to extend the studies of turbulent primary breakup of Refs. 10–21 using similar methods. However, rather than emphasizing the outcomes of the process (e.g., drop sizes and velocities after turbulent primary breakup and the length of penetration of the contiguous liquid jet into the gas) similar to earlier work,[10–21] the present investigation emphasized liquid surface properties, particularly the properties of the ligaments that form at the liquid surface and the mechanism by which drops form from these ligaments during turbulent primary breakup. For completeness, however, other results are reported as well, including new information about drop properties after turbulent primary breakup, the relationship between ligament and drop properties, and rates of drop formation along turbulent liquid surfaces. Similar to most earlier studies of turbulent primary breakup, however, present considerations were limited to turbulent primary breakup of turbulent round and annular (large aspect ratio, nearly plane) free turbulent jets in still air at liquid/gas density ratios where direct aerodynamic effects are small, except as noted earlier. Finally, also similar to past work,[10–21] phenomenological analysis was used to help interpret and correlate the measurements.

The following description of the research begins with consideration of experimental methods. Results are then discussed that address ligament characteristics, ligament breakup mechanisms, ligament breakup properties, ligament and drop diameters at the onset of ligament and drop formation, the locations of the onset of ligament and drop formation, ligament and drop diameters as a function of distance along the liquid surface, drop velocities at the liquid surface, and drop liquid fluxes at the liquid surface based on these velocities.

Experimental Methods

Apparatus

Pressure injection was used to feed either water or ethyl alcohol from cylindrical storage chambers through either round or annular nozzles located at the bottom of the chambers to form turbulent liquid jets directed vertically downward. See Sallam et al.[18] for details about the test apparatus. The annular liquid jets had aspect ratios larger than 20:1 and were used to approximate plane liquid jets to avoid the problems of defining the end effects of finite width plane jets. The storage chambers had the following dimensions: The chamber for the round nozzles had an inside diameter and length of 165 and 305 mm, respectively, whereas the chamber for the annular nozzles had an inside diameter and length of 190 and 305 mm, respectively. All injectors had smooth round entries to avoid the development of cavitating flows and passages having length/hydraulic-diameter ratios larger than 40:1 to insure fully developed turbulent pipe flow at the jet exit.[12,16] The core of the annular liquid jets was well ventilated to prevent collapse of the liquid annulus beyond the jet exit.

The chambers were pressurized with high-pressure air stored in an accumulator having a volume of 0.12 m^3 (allowing pressures up to 1900 kPa) and admitted through a solenoid valve. A baffle at the air inlet prevented mixing between the air and the test liquid. The test liquid was captured in a baffled tub. The nozzle assembly could be traversed vertically with an accuracy of 0.5 mm with a linear bearing system to accommodate rigidly mounted optical instrumentation.

Liquid injection times of 100–400 ms were long compared to both flow development times (6–70 ms) and data accumulation times (less than 100 ns). Flow velocities were calibrated as a function of nozzle pressure drop by the measurement of liquid surface velocities by the use of double-pulse shadowgraphs.

Instrumentation

Measurements were made using single- and double-pulse shadowgraphy and single-pulse off-axis holography. Pulsed shadowgraphy was used for flow visualization and to measure liquid surface velocities, properties at the onset of ligament and drop formation, and drop and ligament properties along the liquid surface. Pulsed holography was used to measure drop liquid flux distributions along the liquid surfaces.

The light sources for shadowgraphy and holography were two frequency-doubled YAG lasers (Spectra Physics Model GCR-130; 532-nm wavelength, 7-ns pulse duration, and up to 300 mJ per pulse optical energy per pulse) that could be controlled to provide pulse separations as small as 100 ns. Images were obtained with an open shutter under darkroom conditions so that the laser pulse duration controlled the exposure time and was short enough to stop the motion of the liquid surface and drops on the film. Different pulse strengths were used to resolve the directional ambiguity of the double-pulse images.

The shadowgraphs were recorded using Polaroid Types 55 and 57 black-and-white film. Data were obtained from the shadowgraphs by mounting them on a computer controlled x–y traversing system (having 1000-nm spatial resolution) and observing the images using a Sony charge-coupled device (CCD) video camera (Model XC-77). The overall arrangement allowed objects (drops and ligaments) having dimensions as small as 5 μm to be observed and as small as 10 μm to be measured with 10% accuracy. Measurements of mean drop velocities were based on the motion of the centroid of the drops; finding these averages was simplified, however, because drop velocity distributions were essentially uniform. Measurement accuracies of the velocities of various points on ligaments were similar to the accuracies of drop velocities. The experimental uncertainties (95% confidence) were smaller than 5 and 20% for mean streamwise and cross stream velocities. Mass-averaged cross stream drop velocities relative to the liquid surface were needed for drop mass flux determinations; they were found when the relative cross stream velocities of 40–400 drops were averaged to obtain experimental uncertainties (95% confidence) smaller than 20%. In all cases, experimental uncertainties were dominated by sampling limitations.

To avoid problems of depth-of-field corrections, single-pulse off-axis holography was used to find drop liquid fluxes at the liquid surface. The arrangement was based on a Spectron Development Laboratories Model HTRC-5000 holographic camera that allowed drops as small as 5-μm diam to be seen and drops as small as 10-μm diam to be measured with 10% accuracy. The holograms were obtained in a darkened room using AGFA 8E75HD-NAH holographic glass plates having a 100 × 125 mm film format. The holograms were reconstructed using a 35-mW HeNe laser with the laser beam collimated to a 50-mm diam and passed through the hologram to provide a real image of the spray. Analysis of the holograms was the same as the shadowgraphs except that x–y traversing of the hologram was supplemented by z traversing (with 5-μm resolution) of the video camera to allow for the three-dimensional nature of the

Table 1 Summary of test conditions for round freejets[a]

Parameter	Water	Ethanol
ρ_f, kg/m^3	997	800
ρ_f/ρ_g	860	690
$\mu_f \times 10^4$, kg/m · s	8.94	16.0
$\sigma \times 10^3$, N/m	70.8	24.0
d, mm	1.9, 4.8, 8.0	4.8
u_0, m/s	3–25	23–30
Re_{fd}	6×10^3–1.36×10^5	5.7×10^4–1.29×10^5
We_{fd}	200–40,000	50,000–300,000
Oh_{fd}	0.0015–0.0024	0.0053
L_c/d	50–300	200–300

[a]Pressure-atomized injection vertically downward in still air at 99 ± 0.5 kPa and 297 ± 0.5 K ($\rho_g = 1.16$ kg/m^3 and $\nu_g = 15.9$ mm^2/s). Round injector with a rounded entry and a passage length-to-diameter ratio greater than or equal to 40:1.

Table 2 Summary of test conditions for annular freejets[a]

Parameter	Value
b, mm	1.00, 3.55, 6.75
u_0, m/s	11.1–31.2
Re_{fd}	2.5×10^4–4.24×10^5
We_{fd}	3,000–151,000
Oh_{fd}	0.00091–0.00336

[a]Annular water jets in air at 100 kPa and 297 ± 0.5 K. Properties of water and air are the same as in Table 1. Annular injector with an annular passage length-to-hydraulic-diameter ratio greater than or equal to 40:1. Hydraulic diameter taken as $2b$.

hologram reconstructions. The rate of drop formation at the liquid surface was obtained by measurement of the volume of the drop liquid within an annular segment defined by the angle between two alignment pins (positioned outside the spray-containing region) and the axis of the liquid jet, with the distance above the mean position of the liquid surface given by the distance the drops moved at their mean relative velocity with respect to the liquid surface for a preselected sampling time. Experimental uncertainties of the liquid flux measurements due to the definition of irregular objects as ellipsoids are difficult to quantify; otherwise, 40–60 sample volumes were evaluated to yield mean radial liquid drop fluxes with experimental uncertainties (95% confidence) less than 30%, mainly dominated by sampling limitations.

Test Conditions

The experiments involved measurements of both round and plane (large aspect ratio annular) liquid turbulent jets. The present tests were limited to water and ethanol injected into still air, however, past work[14–19] concerning round freejets and annular wall jets in still air has shown that effects of variations of liquid and gas properties can be treated effectively by the dimensionless parameters used to summarize the present test results. Present test conditions for round and annular freejets are summarized in Tables 1 and 2, respectively. The Reynolds number range implies that effects of turbulent primary breakup dominated the present results. The small jet exit Ohnesorge numbers imply that direct effects of liquid viscosity on liquid breakup were small.

Results and Discussion

Ligament Characteristics

A typical ligament at the surface of a turbulent liquid jet in still air at NTP (an annular jet in this case) is illustrated in Fig. 1. The ligaments were characterized by the use of an approach similar to a proposal of Merrill and Sarpkaya.[23] The resulting definitions of ligament projected area A_ℓ, ligament length L_ℓ, and ligament angle ϕ, are illustrated in Fig. 1. Given ligament projected area and length, the ligament effective diameter was calculated as follows:

$$d_\ell = A_\ell / L_\ell \tag{1}$$

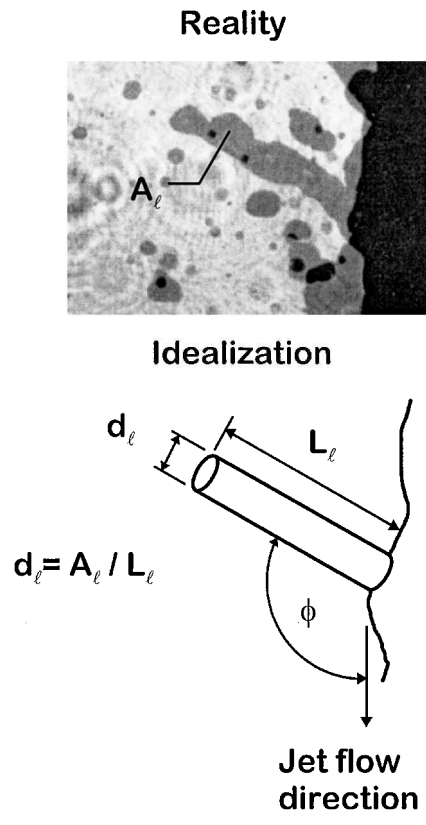

Fig. 1 Definitions of ligament projected area, ligament diameter, ligament length, and ligament angle.

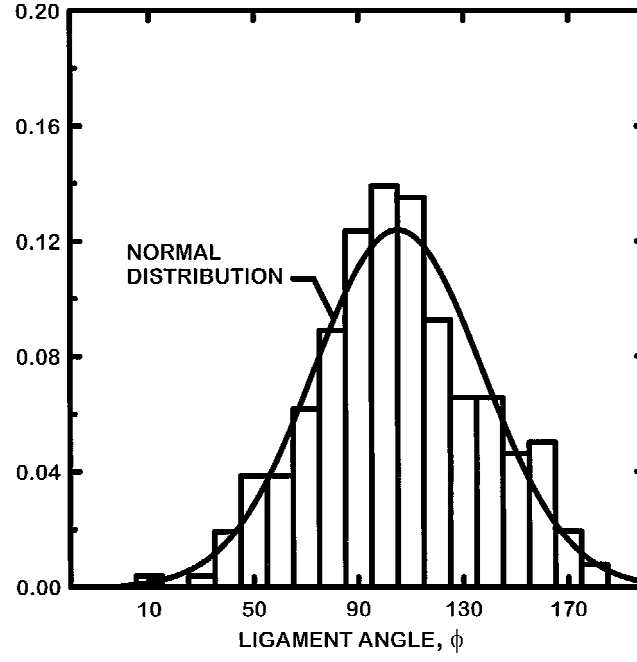

Fig. 2 Probability density distribution of ligament angle for round and annular turbulent freejets in still air.

Measurements of 250 ligaments at the surfaces of round and annular free turbulent jets in still air yielded the probability density distribution of ligament angle illustrated in Fig. 2. The probability density distribution of ligament angle was roughly Gaussian, with a mean angle of 105 deg and a standard deviation of roughly 32 deg. In view of the relatively large standard deviation of the probability density distribution illustrated in Fig. 1, these results indicate that the ligaments are nearly randomly oriented, representative of the

random nature of a turbulent process. This behavior also suggests small aerodynamic effects on the motion of ligaments for present test conditions because aerodynamic effects would be expected to deflect ligaments toward the jet exit to yield values of ϕ generally larger than 90 deg. This behavior is in agreement with past observations of small aerodynamic effects on turbulent primary breakup for present test conditions.

Ligament Breakup Mechanisms

Two mechanisms of ligament breakup were observed, as follows: 1) ligament tip (Rayleigh) breakup and 2) ligament base breakup. Typical shadowgraphs of ligament tip and ligament base breakup are illustrated in Figs. 3 and 4, respectively. Ligament tip breakup was the dominant drop formation mechanism during turbulent primary breakup and was observed roughly 90% of the time. In this case, ligament breakup occurred at the tip of the ligament, similar to classical Rayleigh breakup, where the ligaments act like liquid jets emerging from the liquid surface. Ligament tip breakup yielded drop/ligament-diameter ratios at the time of drop formation from the tip of the ligament close to 1.9, which was proposed by Tyler[24] to be roughly the diameter ratio for Rayleigh breakup of liquid jets.

The second mechanism of drop formation, ligament base breakup, was observed less than 10% of the time and involved breakup of the ligament at its base due to turbulent cross stream liquid velocity fluctuations that change the flow direction at the base of the ligament before Rayleigh breakup can occur at the ligament tip. This mechanism was characterized by the formation of large, irregular, ligamentlike drops and yielded larger drop/ligament diameter ratios than those associated with conditions where Rayleigh breakup occurs at the tip of the ligament.

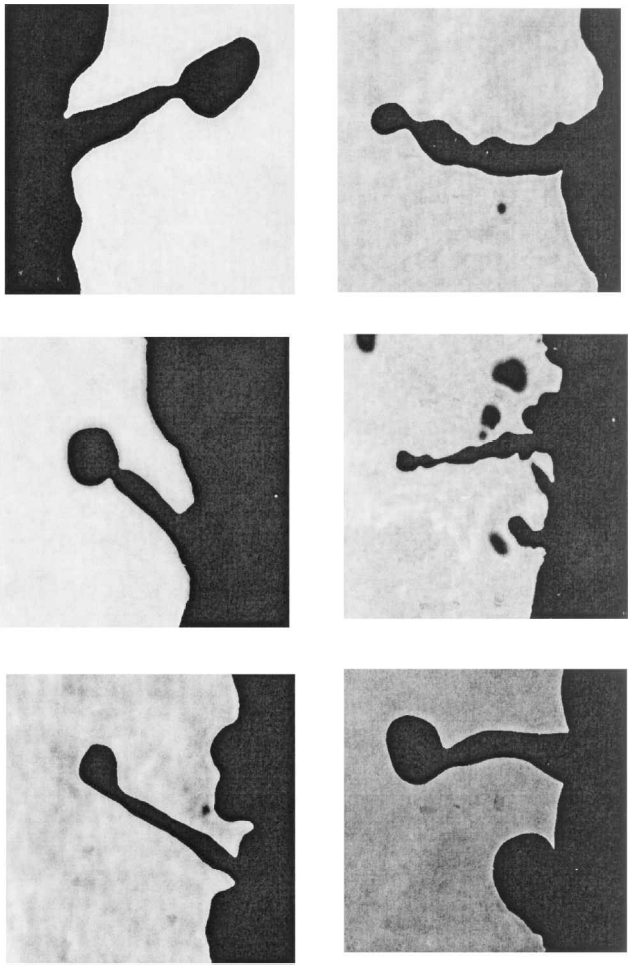

Fig. 3 Typical shadowgraphs of ligament tip (Rayleigh) breakup at the surface of round and annular turbulent freejets in still air.

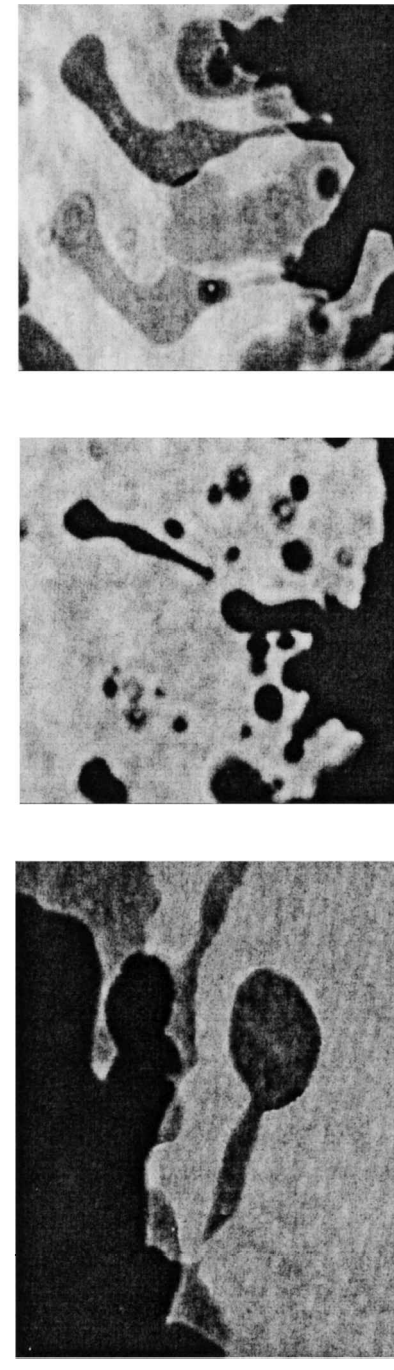

Fig. 4 Typical shadowgraphs of ligament base (turbulent) breakup at the surface of round and annular turbulent freejets in still air.

Ligament Breakup Properties

The probability density distribution of drop/ligament-diameter ratios at the time of drop formation for a given surface condition was roughly Gaussian with a mean value of 2.1 and a standard deviation of 0.78. This result helps to quantify the conclusion that ligament tip breakup was the dominant mechanism of drop formation during present observations of turbulent primary breakup. In particular, ligament breakup processes mainly yielded values of drop/ligament diameter near the value of 1.9 anticipated for Rayleigh breakup of a ligament at its tip,[24] rather than the larger values (greater than three) typical of the large ligamentlike drops formed by the ligament base breakup mechanism. Finally, the large standard deviation of drop/ligament-diameter ratio reflects the large variations of flow properties present for a random process such as turbulent primary breakup, compared to the precisely established conditions used to observe for Rayleigh breakup where drops form at the tip of laminar liquid jets.

Measurements of the ligament slenderness ratio at breakup (i.e., the ligament length/diameter ratio at the instant when a drop forms at the tip of the ligament) provided another useful parameter to evaluate whether drop formation at the tips of the ligaments corresponds to a conventional Rayleigh breakup process or not. The theoretical prediction of this length/diameter ratio based on analysis by Weber[25] is given, as follows:

$$\frac{L_\ell}{d_\ell} = \ell n\left[\frac{d_\ell}{(2\delta)}\right]\left(\frac{3We_{f\ell}}{Re_{f\ell}} + We_{f\ell}^{\frac{1}{2}}\right) \tag{2}$$

In Eq. (2), δ is the amplitude of the disturbance at the base of the ligament that eventually grows to separate a drop from the tip of the ligament. The parameter $\ell n[d_\ell/(2\delta)]$ must be determined experimentally; for example, Weber[25] reported a value of 12 for this parameter. The ligament velocity u_ℓ, needed to find $We_{f\ell}$ and $Re_{f\ell}$ was taken to be equal to the cross stream velocity of the ligament tip because the streamwise velocities at the base and tip of ligaments were nearly equal. The cross stream velocities of the ligaments were also nearly the same as the cross stream velocities of drops just after turbulent primary breakup, that is, $0.055\,u_0$ (Ref. 18). Finally, for present conditions, $We_{f\ell}/Re_{f\ell} \ll We_{f\ell}^{1/2}$, and the first term in Eq. (2) can be ignored. The remaining ligament properties in Eq. (2) could be measured directly from the present test data, yielding the experimental uncertainties discussed earlier.

Present measurements of ligament slenderness ratios, L_ℓ/d_ℓ, for round and annular (nearly plane)turbulent freejets are plotted in Fig. 5 as a function of $We_{f\ell}$, as suggested by Eq. (2). The measurements are reasonably well correlated in this manner, yielding a best fit of the data, which are illustrated in Fig. 5, as follows:

$$L_\ell/d_\ell = 3.9We_{f\ell}^{0.32} \tag{3}$$

The standard deviation of the power and coefficient of Eq. (3) are 22 and 7%, respectively, and represent the correlation coefficient of the fit of 0.86. As a result, the power of $We_{f\ell}$ in Eq. (3) is not statistically different from the theoretical value of one-half in Eq. (2); therefore, the data were refitted according to the theoretical result of Weber[25] from Eq. (2), to yield the following correlation, which is also illustrated in Fig. 5:

$$L_\ell/d_\ell = 3.2We_{f\ell}^{\frac{1}{2}} \tag{4}$$

Equation (4) suggests a value of 3.2 for the parameter, $\ell n[d_\ell/(28)]$, in contrast to the value of 12 reported earlier by Weber.[25] This result indicates $d_\ell/\delta \approx 50$ for ligament breakup, which implies a disturbance of the ligament diameter at its base on the order of 2% of the ligament diameter itself, for subsequent Rayleigh breakup at the ligament tip.

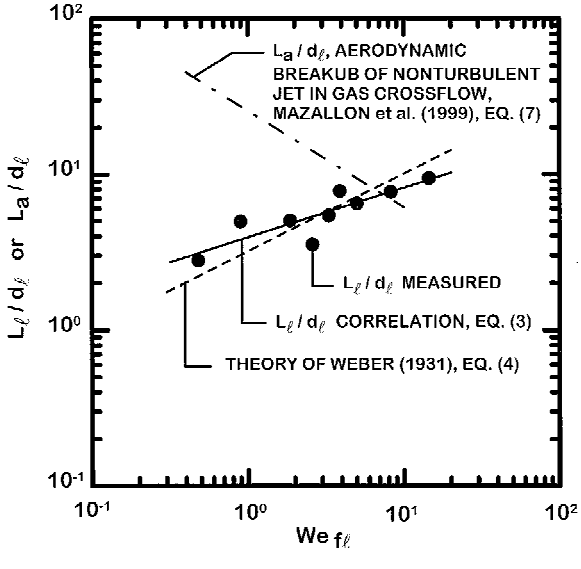

Fig. 5 Ligament slenderness ratios at breakup as a function of the Weber number for 1) turbulent primary breakup along round and annular turbulent freejets in still air, and 2) aerodynamic breakup of nonturbulent round ligaments in crossflow.

Another important issue is the extent that aerodynamic effects potentially influence ligament breakup, compared to conventional Rayleigh breakup, to form a drop at the tip of the ligament, for example, to determine whether aerodynamic breakup of the ligament tip occurs sooner than Rayleigh breakup at the ligament tip. This was done by exploitation of the results of Mazallon et al.[26] concerning the breakup of nonturbulent round liquid jets in gaseous crossflows (noting that the ligaments themselves do not exhibit significant levels of internal turbulence based on their relatively smooth surfaces). This was done, as before, by approximation of ligament breakup by a liquid jet escaping normally from the liquid surface with a jet velocity equal to the relative cross stream drop velocities after breakup, that is, $0.055u_0$ (Ref. 18). In addition, the ligament as a jet is subjected to a crossflow of air at NTP having a velocity equal to the liquid surface velocity of the liquid jet u_0 (Ref. 17). The aerodynamic ligament breakup time was then obtained as the breakup time of nonturbulent round liquid jets in crossflow from Mazallon et al.,[26] as follows:

$$t_a\Big/\left[d_\ell(\rho_f/\rho_g)^{\frac{1}{2}}\Big/u_0\right] = 8.76\left(\rho_g d_\ell u_0^2\Big/\sigma\right)^{-0.62} \tag{5}$$

The aerodynamic ligament breakup length $L_a = 0.055u_0t_a$, then becomes

$$L_a/d_\ell = 0.0132(\rho_f/\rho_g)^{1.12}We_{f\ell}^{-0.62} \tag{6}$$

For water jets injected into air at NTP, Eq. (6) becomes

$$L_a/d_\ell = 25We_{f\ell}^{-0.62} \tag{7}$$

This is plotted in Fig. 5. It is evident that except for a few test points, the present measurements largely involve conditions where Rayleigh breakup occurs at the ligament tip, that is, at conditions where the ligament length required for Rayleigh breakup at the ligament tip is smaller than the ligament length required for aerodynamic breakup at the tip of the ligament. Notably, this behavior is also in agreement with the appearance of the ligament breakup process that was typified by the formation of the drops at the tips of the ligaments having a diameter roughly twice the ligament diameter, as discussed in connection with Figs. 3 and 4 and supported by measurements of d_ℓ and the SMD of drops formed by turbulent primary breakup to be discussed subsequently.

Ligament and Drop Diameters at Onset

Analogous to earlier findings concerning drop sizes at the onset of turbulent primary breakup along the surfaces of turbulent liquids in still gases,[17,21] ligament diameters at the onset of ligament formation were found by equating the kinetic energy (relative to its surroundings) of a characteristic eddy of a given characteristic size λ_i to the surface tension energy required to start the formation of a ligament of this characteristic size. To find the onset eddy size, the critical geometry of the start of ligament formation was taken to be a hemisphere having a diameter proportional to λ_i because this configuration involves the maximum surface tension energy per unit surface area of any configuration present during ligament formation. Then, equating the kinetic energy of the eddy to the surface tension energy of the hemispherical distortion of the liquid surface results in

$$\rho_f v_{\lambda i}^2 \lambda_i^3 \sim \sigma\lambda_i^2 \tag{8}$$

Ligament sizes at the onset of ligament formation, and generally throughout the region where ligaments form for present test conditions, are larger than the microscales (Kolmogorov scales) of the liquid turbulence; instead, they fall within the inertial range of the turbulence. For these conditions, eddy sizes and characteristic eddy velocities are related as follows[27]:

$$v_\lambda \sim \bar{v}_0'(\lambda/\Lambda)^{\frac{1}{3}} \tag{9}$$

where Λ is the cross stream integral length scale of the flow at the jet exit. Similar to past work,[14] the cross stream integral length scale was taken to be $\Lambda = d_h/8$, based on Laufer's measurements of the properties of fully developed turbulent pipe flow. (See Hinze[28] and references cited therein.) Combination of Eqs. (8) and (9), along with the assumption that the ligament diameter at the onset of ligament formation is proportional to the characteristic eddy size at the onset of ligament formation, $d_{\ell i} \sim \lambda_i$, an expression for the ligament diameter at the onset of ligament formation is obtained, as follows:

$$d_{\ell i}/\Lambda = C_{\ell i}(u_0/\bar{v}_0')^{\frac{6}{5}} We_{f\Lambda}^{-\frac{3}{5}} \tag{10}$$

where $C_{\ell i}$ is an empirical constant that should have a value on the order of unity.

Based on the discussion of Figs. 3 and 4, drop breakup at the tips of ligaments dominates drop formation during turbulent primary breakup. This involves Rayleigh breakup at the ligament tip, which implies that drop diameters at the onset of drop formation should be proportional to ligament diameters at the onset of ligament formation, based on the results of Tyler.[24] Then, the assumption that the SMD at the onset of drop formation (SMD_i) is also proportional to the ligament diameter at the onset of ligament formation results in

$$\mathrm{SMD}_i/\Lambda = C_s(d_{\ell i}/\Lambda) \tag{11}$$

where C_s should be an empirical constant on the order of unity.

Present measurements of the ligament diameter at the onset of ligament formation $d_{\ell i}$ and SMD_i are plotted as a functions of $We_{f\Lambda}$, as suggested by Eqs. (10) and (11), in Fig. 6. The scatter of the measurements is generally within the scatter anticipated based on experimental uncertainties. The power of $We_{f\Lambda}$ for the correlation of $d_{\ell i}/\Lambda_i$ is not $-\frac{3}{5}$, as suggested by Eq. (10), however, and can be represented better by the following empirical fit that is shown in Fig. 6:

$$d_{\ell i}/\Lambda = 700 We_{f\Lambda}^{-0.94} \tag{12}$$

The standard deviations of the power and coefficient in Eq. (12) are 12 and 15%, respectively, and the correlation coefficient of the fit is 0.92. The reduction of the power of $We_{f\Lambda}$ from $-\frac{3}{5}$ (or -0.60) in Eq. (10) to -0.94 in Eq. (12) is marginally statistically significant, but is not large in view of the approximations used to develop the correlating expression and the experimental uncertainties of the measurements. Notably, correlation of SMD_i/Λ at the onset of drop breakup along turbulent round liquid jets in still gases at NTP also exhibited a decrease of the value of power of $We_{f\Lambda}$ (in that case, from $-\frac{3}{5}$ (or -0.60) to -0.75).[14] Finally, the coefficient of Eq. (12) is relatively large, but this can be anticipated from Eq. (10) if $C_{\ell i}$ is on the order of unity because $(u_0/\bar{v}_0')^{6/5}$ is large for fully developed turbulent pipe flow, that is, $u_0/\bar{v}_0' \approx 33$ for the present flow.[28] In addition, the increased negative power of $We_{f\Lambda}$ compared to the phenomenological theory estimate of Eq. (10) should also tend to increase the value of the coefficient of Eq. (12).

The correlation of SMD_i/Λ essentially agrees with Eq. (11) within experimental uncertainties, to yield the following empirical fit shown on the plot illustrated in Fig. 6:

$$\mathrm{SMD}_i/\Lambda = 1.24(d_{\ell i}/\Lambda) \tag{13}$$

The standard deviation of the coefficient of Eq. (13) is 12%, whereas the correlation coefficient of this fit is comparable to the fit of $(d_{\ell i}/\Lambda)$ in Eq. (12), namely, 0.95. Thus, C_s in Eq. (11) is on the order of magnitude of unity, as expected, and these results are consistent with the hypothesis that drop formation mainly involves Rayleigh breakup at the tips of ligaments to form drops.

Finally, the correlation of SMD_i/Λ for turbulent primary breakup along the free surface of turbulent liquid wall jets in still gases, due to Dai et al.,[20] is also illustrated in Fig. 6. These drop sizes are similar to the results for round and plane turbulent freejets but are somewhat larger. This behavior is not unanticipated, however, because turbulence far from the turbulence-generating surface of wall jets is expected to have larger scales than turbulence along the surface of freejets, which initially is produced by flow properties near the surface of the injector passages.

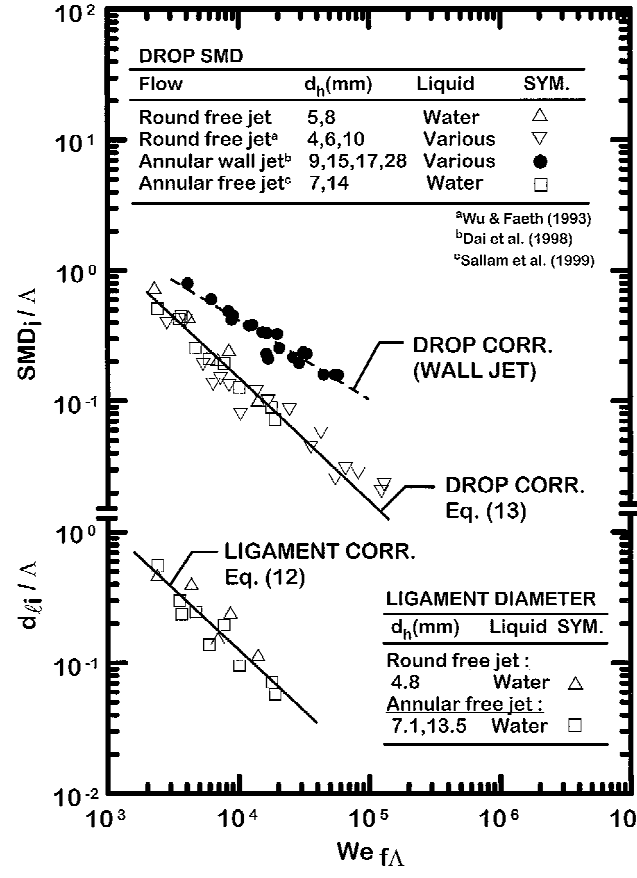

Fig. 6 Ligament and drop diameters at the onset of their formation along the surfaces of round and annular turbulent freejets in still air and drop sizes at the onset of drop formation along the surface of plane turbulent wall jets in still air, as functions of the Weber number.

Locations of Onset of Ligament and Drop Formation

The location of the onset of ligament formation follows from the estimation of the size of ligaments at the onset of ligament formation that was just discussed. Recall that a ligament is assumed to be created by an eddy of corresponding size. Thus, it is reasonable to assume that the time required for the onset of ligament formation is proportional to the characteristic eddy time[28]:

$$t_{\ell i} \sim d_{\ell i}/v_{\ell i} \tag{14}$$

Then, the distance moved in the streamwise direction from the jet exit as the flow develops for the characteristic eddy time is given by

$$x_{\ell i} \sim u_0 t_{\ell i} \tag{15}$$

Similar to earlier considerations of ligament diameter at the onset of ligament formation, from Eq. (9), eddy velocities and sizes at the onset of ligament formation are related as follows:

$$v_{\ell i} \sim \bar{v}_0'(d_{\ell i}/\Lambda)^{\frac{1}{3}} \tag{16}$$

Then, when Eqs. (15) and (16) are substituted into Eq. (14) and distance normalized by the radial integral length scale, similar to earlier analysis of onset conditions for drop formation,[14] the length required to initiate the onset of ligament formation becomes

$$x_{\ell i}/\Lambda \sim (u_0/\bar{v}_0')(d_{\ell i}/\Lambda)^{\frac{2}{3}} \tag{17}$$

Finally, by substitution for the diameter of the ligaments at the onset of ligament formation $d_{\ell i}/\Lambda$, from Eq. (10) into Eq. (17), an

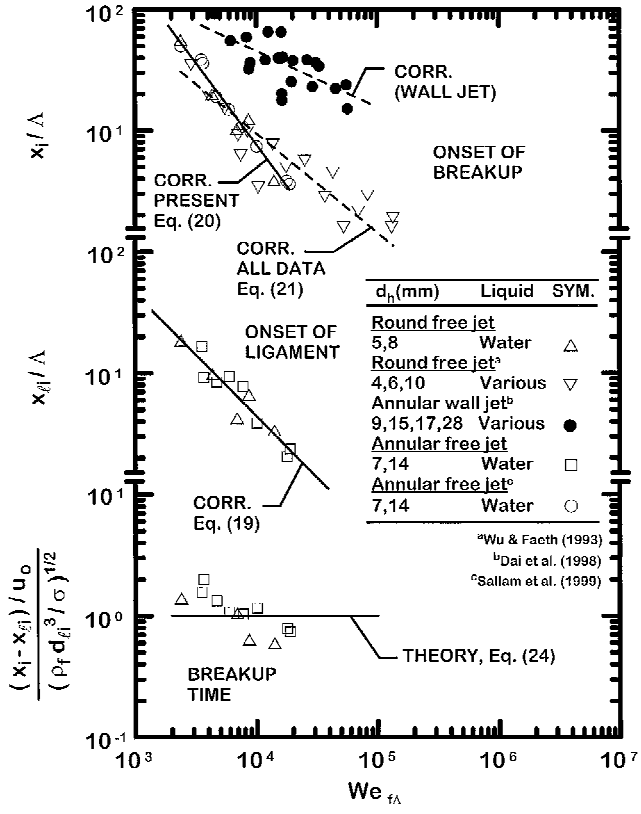

Fig. 7 Length to initiate ligament formation, length to initiate drop formation, and time of ligament breakup as functions of the Weber number for round and annular freejets in still air.

expression for $x_{\ell i}/\Lambda$ is obtained in terms of jet exit conditions, as follows:

$$x_{\ell i}/\Lambda = C_{xi}(u_0/\bar{v}_0')^{\frac{9}{5}} We_{f\Lambda}^{-0.4} \tag{18}$$

where C_{xi} is an empirical parameter that should have a value on the order of unity that involves the various constants of proportionality in Eqs. (14–17).

Present measurements of the locations of the onset of ligament formation along the surfaces of round and plane (annular) turbulent liquid jets in still gases at NTP are plotted in Fig. 7, as suggested by Eq. (18). The best fit correlation of the measurements of $x_{\ell i}/\Lambda$, according to the variables of Eq. (18), are also shown in Fig. 7; this correlation is given by

$$x_{\ell i}/\Lambda = 49{,}600 We_{f\Lambda}^{-1.01} \tag{19}$$

The standard deviation of the power and coefficient of Eq. (19) are 8 and 6%, respectively, and the correlation coefficient of the fit is 0.95, which is quite good. Similar to the earlier correlation of $d_{\ell i}/\Lambda$ in Eq. (12), the power of $We_{f\Lambda}$ in Eq. (19) is significantly more negative than the theoretical expression of Eq. (18), but this is not unreasonable due to the approximations used to develop the correlating expression. Finally, the coefficient of Eq. (19) is unusually large, but this can be anticipated from Eq. (18) if C_{xi} is on the order of unity because $(u_0/\bar{v}_0')^{9/5}$ is large for fully developed turbulent pipe flow, as noted earlier.[28]

The development of a correlating expression for the location of the onset of drop formation along the surface differs somewhat from the analysis to find the location of the onset of ligament formation. This comes about because the characteristic eddy time of Eq. (14) is significantly smaller than the Rayleigh breakup time of ligaments for present conditions, and the Rayleigh breakup time controls the time, thus the streamwise distance, required to reach the onset of drop formation. In addition, the Rayleigh breakup time is not significantly influenced by liquid viscosity for present conditions similar to earlier analysis to find the location of the onset of drop formation.[14] As a result, phenomenological analysis to find x_i/Λ is unchanged from Wu et al.[14] and yields the following correlating expression, plotted in Fig. 7, based on present measurements for round turbulent liquid jets in still gases and earlier measurements for annular (nearly plane) turbulent liquid jets in still gases due to Sallam et al.[21]:

$$x_i/\Lambda = 2{,}000{,}000 We_{f\Lambda}^{-1.36} \tag{20}$$

The standard deviations of the power and coefficient of Eq. (20) are 5 and 4%, respectively, and the correlation coefficient of the fit is 0.98, which is quite good. If the measurements of Wu and Faeth[15] for round turbulent jets in still gases are added to the data set, which increases the range of $We_{f\Lambda}$ by roughly an order of magnitude, a new correlating expression, also plotted in Fig. 7, is obtained, as follows:

$$x_i/\Lambda = 18{,}000 We_{f\Lambda}^{-0.82} \tag{21}$$

The standard deviations of the power and coefficient of Eq. (21) are 8 and 6%, respectively, and the correlation coefficient of the fit is 0.92. The reason for the change of slope of Eqs. (20) and (21) is not known; it is recommended that whichever correlation gives the largest value of x_i/Λ be used, pending resolution of the variation of behavior near the ends of the test range in Fig. 7.

Similar to the earlier correlations of SMD_i/Λ in Eq. (13) [after substitution of $d_{\ell i}/\Lambda$, in this expression, from Eq. (10)], it is evident that the powers of $We_{f\Lambda}$ in Eqs. (20) and (21) are significantly more negative than the theoretical expression of Eq. (13). As before, however, this is not unreasonable due to the approximations used to develop the correlating expression. Finally, the coefficients of Eqs. (20) and (21) are unusually large, which can be anticipated from the original analysis,[14] which shows that this coefficient is proportional to $(u_0/\bar{v}_0')^{9/5}$ which is large for fully developed turbulent pipe flow, as already discussed in connection with Eq. (19).

Finally, the distance between the onset of ligament formation and the onset of drop formation should be proportional to the distance convected by the ligament responsible for these two conditions for its Rayleigh breakup time, or

$$x_i - x_{\ell i} \sim u_0 t_{ri} \tag{22}$$

From the results of Weber,[25] given that effects of liquid viscosity on the Rayleigh breakup time are small, as before, the Rayleigh breakup time of the critical ligament that first appears at the liquid surface, and subsequently is the first ligament to form a drop, is given as follows:

$$t_{ri} \sim \left(\rho_f d_{\ell i}^3/\sigma\right)^{\frac{1}{2}} \tag{23}$$

Combination of Eqs. (22) and (23) then yields the following expression for the normalized Rayleigh breakup length of the critical ligament that is responsible for both the onset of ligament and drop formation along the surface:

$$\frac{(x_i - x_{\ell i})}{\left[u_0\left(\rho_f d_{\ell i}^3/\sigma\right)^{\frac{1}{2}}\right]} = C_{xr} \tag{24}$$

The ratio of critical ligament breakup time to its Rayleigh breakup time, as given by Eq. (24), is also plotted in Fig. 7. Present measurements of round and plane (annular) turbulent freejets in still gases are considered in Fig. 7. The measurements suggest a systematic reduction of the ligament/Rayleigh breakup time ratio with increasing $We_{f\Lambda}$, but this effect is not large and yields $C_{xr} = 1.08$ with a standard deviation of 39%. In view of the complexities of turbulent primary breakup along turbulent liquid surfaces in still gases, this result also provides considerable support for the hypothesis that ligaments are undergoing Rayleigh breakup at their tips as the main mechanism controlling both maximum ligament lengths and drop sizes after breakup, due to the turbulent primary breakup process.

Ligament and Drop Sizes Along the Surface

An expression for the variation of ligament diameter as a function of distance from the jet exit due to effects of turbulent primary breakup for annular and round freejets was developed. This was accomplished by the use of methods used earlier for the variation of the SMD of drops formed by turbulent primary breakup for both round freejets[14] and annular wall jets.[18] This approach was adopted after the close relationship between the diameters of ligaments that are just forming drops at a point (the most prominent ligaments at a point due to their length) and the corresponding diameters of drops formed by Rayleigh breakup of these ligaments was noted. This was discussed in connection with Eqs. (10) and (11). This was done with consideration given to the convection of a ligament along the surface of a turbulent liquid jet for the Rayleigh breakup time required to form a full-length ligament that is ready to produce a drop. Weber[25] showed that the Rayleigh breakup time of a liquid jet having a diameter of d_ℓ, and, thus, a ligament of similar size under present assumptions, is as follows:

$$t_r \sim \left(\rho_f d_\ell^3/\sigma\right)^{\frac{1}{2}} + 3\mu_f d_\ell/\sigma \tag{25}$$

where the second term on the right-hand side of Eq. (25) accounts for the effects of liquid viscosity to increase the Rayleigh breakup time. For present conditions, the viscous term in Eq. (25) is small and can be ignored, as noted earlier. This term, however, could be a factor for very viscous liquids at conditions where the Ohnesorge numbers of the ligaments, and the drops formed by ligament breakup, are large.[14] Under present approximations, however, Eq. (25) becomes

$$t_r \sim \left(\rho_f d_\ell^3/\sigma\right)^{\frac{1}{2}} \tag{26}$$

which is independent of the ligament velocity. Then, under the assumption that the ligament is simply convected along the liquid surface for the ligament breakup time, the location where a ligament having a particular diameter reaches its full length is given by

$$x \sim u_0 t_r \tag{27}$$

Finally, substitution of Eq. (26) into Eq. (27) and normalization of the streamwise distance by the radial integral scale Λ, similar to that of Wu et al.,[14] yields the following expression for the variation of d_ℓ/Λ with distance from the jet exit:

$$d_\ell/\Lambda = C_{\ell x}\left[x\Big/\left(\Lambda We_{f\Lambda}^{\frac{1}{2}}\right)\right]^{\frac{2}{3}} \tag{28}$$

where $C_{\ell x}$ is a constant of proportionality that should be on the order of unity. Ligaments of interest here are those that are forming drops at a particular distance from the jet exit; therefore, the ligament diameters increase with increasing distance from the jet exit because larger ligaments require a longer time to develop and break up, as indicated by Eq. (26) and, thus, a larger distance from the jet exit as indicated by Eq. (27).

Present measurements of ligament diameters along the surface of turbulent round and annular (nearly plane) freejets in still gases are plotted in Fig. 8, as suggested by Eq. (28). Limits that give the onset of turbulent primary breakup along the surface, as well as the liquid column breakup length, are also shown in Fig. 8 to help define the portion of the liquid surface where turbulent primary breakup can recur. These limits do not correlate in the same manner as d_ℓ/Λ and appear as bands rather than lines as a result. The best fit correlation of d_ℓ/Λ according to the variables of Eq. (28), shown in Fig. 8, is given by

$$d_\ell/\Lambda = 0.38\left[x\Big/\left(\Lambda We_{f\Lambda}^{\frac{1}{2}}\right)\right]^{0.61} \tag{29}$$

The standard deviations of the power and coefficient of Eq. (29) are 9 and 8%, respectively, and the correlation coefficient of the fit is 0.95, which is quite good. The difference between the best fit power in Eq. (29) and the theoretical power in Eq. (28) is not statistically significant; therefore, this fit was recorrelated by the use of the theoretical power to obtain the following expression:

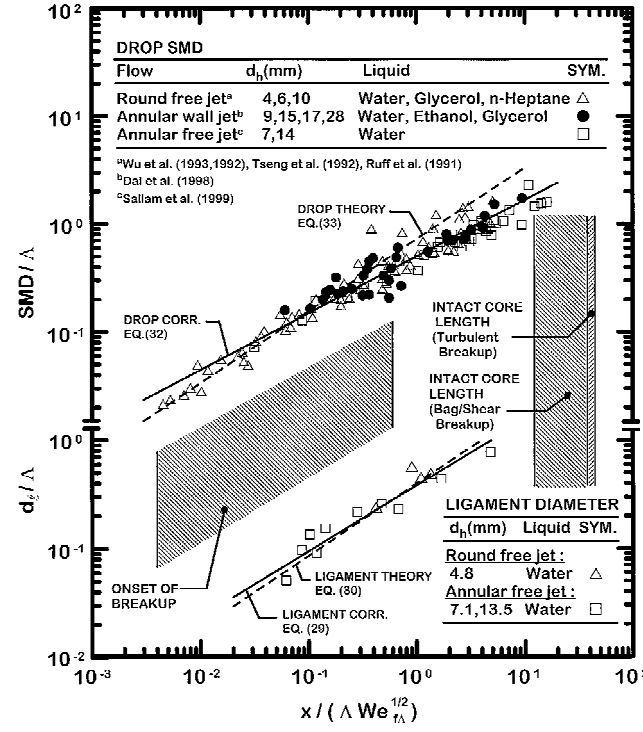

Fig. 8 Ligament and drop diameters for round and annular freejets and drop diameters for plane wall jets in still air, as a function of normalized streamwise distances.

$$d_\ell/\Lambda = 0.40\left[x\Big/\left(\Lambda We_{f\Lambda}^{\frac{1}{2}}\right)\right]^{\frac{2}{3}} \tag{30}$$

The standard deviation of the coefficient of Eq. (30) is 10%. Given the general form of the theoretical expression of Eq. (28), it is evident that the order of magnitude of the coefficient in Eq. (30) is unity, as anticipated. Taken together, the results of Eqs. (29) and (30) help to support the physical ideas used to develop these expressions.

Next, based on the ideas used to relate SMD_i to $d_{\ell i}$, discussed in connection with Eq. (13), drop diameters resulting from Rayleigh breakup of ligaments should be roughly twice the diameters of the most prominent ligaments at the same location. Thus, from Eq. (13), this behavior implies the following expression for the variation of the SMD after turbulent primary breakup as a function of distance from the jet exit:

$$\mathrm{SMD}/\Lambda = C_{sx}\left[x\Big/\left(\Lambda We_{f\Lambda}^{\frac{1}{2}}\right)\right]^{\frac{2}{3}} \tag{31}$$

where C_{sx} is a constant of proportionality that should be on the order of unity.

Present measurements of SMD after turbulent primary breakup along the surface of turbulent round and plane (annular) freejets in still gases are plotted, as suggested by Eq. (31), in Fig. 8. The best fit correlation of SMD/Λ according to the variables of Eq. (31), shown in Fig. 8, is given by

$$\mathrm{SMD}/\Lambda = 0.5\left[x\Big/\left(\Lambda We_{f\Lambda}^{\frac{1}{2}}\right)\right]^{0.53} \tag{32}$$

The standard deviations of the power and coefficient of Eq. (32) are 2 and 3%, respectively, whereas the correlation coefficient of the fit is 0.97, which is quite good. In this case, the difference between the powers of the variable on the right-hand sides of Eqs. (31) and (32) is statistically significant. This suggests a physical reason for the drop diameters, after primary breakup, not increasing as rapidly as ligament diameters with increasing streamwise distance from the

jet exit, as anticipated by Rayleigh breakup of ligaments. A possible explanation of this behavior could be merging of turbulent primary breakup and aerodynamic secondary breakup of drops as they break up at the tips of ligaments, as discussed by Wu and Faeth.[15] Supporting evidence for this behavior is provided by the results plotted in Fig. 5, which suggests possible merging of turbulent primary breakup and aerodynamic secondary breakup for the longer ligaments observed during the present investigation, which are found as the largest values of $x/(\Lambda We_{f\Lambda}^{1/2})$ are approached in Fig. 8.

Even though it requires a greater degree of forcing of the power of independent variable in Fig. 8, it also is of interest to examine estimates of SMD/Λ as a function of streamwise distance, based on the theoretical correlation of Eq. (31). Completing the best fit correlation of the theory, which is also plotted in Fig. 8, yields

$$\mathrm{SMD}/\Lambda = 0.72\left[x \Big/ \left(\Lambda We_{f\ell}^{\frac{1}{2}}\right)\right]^{\frac{2}{3}} \tag{33}$$

The standard deviation of the coefficient of Eq. (33) is 5%. Given the general form of Eq. (31), it is evident that the order of magnitude of the coefficient of Eq. (33) is unity and that the value of this coefficient is roughly twice the value of the coefficient of Eq. (30), both as expected for a Rayleigh breakup of process of ligaments to form drops. Thus, the results of Eqs. (30) and (33) also help to support the physical ideas used to develop these expressions.

Drop Velocities After Turbulent Primary Breakup

Earlier work showed that drop velocities after turbulent primary breakup were independent of drop size[21]; therefore, drop velocities are fully described by a single moment that will be taken to be mass-weighted (or Favre-averaged) velocities in the following. Two components of drop velocity after turbulent primary breakup were of major interest for present considerations, $\tilde{u}$ and $\tilde{v}$. (See Sallam et al.[18,21] for information about the other velocity properties of the drops formed by turbulent primary breakup along turbulent liquid surfaces in still gases.)

Mean streamwise and relative cross stream drop velocities are functions of the normalized distance from the jet exit. First, results for round and annular turbulent free liquid jets from Sallam et al.[18] and for annular wall jets from Dai et al.[19] show that normalized drop velocities are essentially the same for these flows. Next, the most effective normalizing velocity is the mean streamwise liquid surface velocity $\bar{u}_s$. In addition, the mean liquid surface velocity for round and plane free liquid jets is essentially independent of distance along the jet, except for a region involving $x/d_h < 4$, where the surface velocities are slightly retarded due to drag effect of the injector passage walls.[14] Beyond this region,

$$\bar{u}_s/u_0 = 0.89 \tag{34}$$

with a standard deviation of 5% based on present measurements, in general agreement with earlier measurements of mean liquid surface velocities of free turbulent liquid jets in still gases.[18,19,21] Next, all of these measurements indicate

$$\tilde{u}/\bar{u}_s = 0.89 \tag{35}$$

with a standard deviation of 4% over the length of the free liquid jets, except for the region near the jet exit mentioned earlier. Finally, cross stream drop velocities relative to the liquid surface, which are essential for prescribing the mass flux of drop liquid relative to the liquid surface, exhibit the same streamwise variation for round and annular freejets, and for plane wall jets, as follows:

$$\tilde{v}_r/\bar{u}_s = 0.055,\ x \Big/ \left(\Lambda We_{f\Lambda}^{\frac{1}{2}}\right) < 1 \tag{36}$$

$$\tilde{v}_r/\bar{u}_s = 0.055\left[x \Big/ \left(\Lambda We_{f\Lambda}^{\frac{1}{2}}\right)\right]^{-0.78}, \qquad x \Big/ \left(\Lambda We_{f\Lambda}^{\frac{1}{2}}\right) > 1 \tag{37}$$

The value of $\tilde{v}_r/\bar{u}_s$ given by Eq. (36) has a standard deviation of 21%. The standard deviations of the power and coefficient in Eq. (37) are 24 and 9%, respectively, whereas the correlation coefficient of the fit of this equation is 0.90. The value of $\tilde{v}_r/\bar{u}_s = 0.055$ near the jet exit, or, correspondingly, the value of $\tilde{v}_r/u_0 = 0.050$, is comparable to, but somewhat larger than, the rms cross stream velocity fluctuations of fully developed turbulent pipe flow not too near the wall.[28] This might be expected for conditions where surface tension forces at the liquid surface are relatively small compared to the momentum of the eddies responsible for creating ligaments and drops as part of the turbulent primary breakup process.

Liquid Breakup Rates Due to Turbulent Primary Breakup

The last liquid surface property that was studied during the present investigation was the flux of liquid drops relative to the liquid surface due to turbulent primary breakup along the liquid surface, or $\dot{m}_f''$. The objective was to extend earlier considerations of this property for turbulent primary breakup of round liquid jets due to Sallam et al.[21] to turbulent primary breakup of plane (or annular) liquid jets. Present measurements were summarized in the same manner as those made by Sallam et al.,[21] by defining a liquid surface breakup efficiency factor ε, as follows:

$$\varepsilon = \dot{m}_f''/(\rho_f \tilde{v}_r) \tag{38}$$

where the limit $\varepsilon = 1$ represents conditions where liquid drops form in a continuous manner over all of the projected liquid jet surface area. The actual appearance of liquid surfaces during turbulent primary breakup, particularly as the result of Rayleigh breakup at the tips of growing ligaments along the surface, however, suggests that, usually, $\varepsilon < 1$, if not $\ll 1$. Naturally, it is expected that $\varepsilon \approx 0$ near the onset of drop formation due to turbulent primary breakup.

Present measurements of ε for turbulent primary breakup of annular (nearly plane) freejets in still air at NTP are illustrated in Fig. 9, along with the earlier measurements of Sallam et al.,[21] for turbulent primary breakup of round liquid jets in still air at NTP. The independent variable used on this plot is $x/(\Lambda We_{f\Lambda}^{1/2})$, which was the characteristic streamwise variable used to correlate both the SMD and the value of $\tilde{v}_r$ of drops after turbulent primary breakup as a function of distance along the liquid surface, as discussed in connection with Fig. 8 and Eqs. (36) and (37). In all cases, the hydraulic diameter was used to find Λ. As discussed earlier, values of $\tilde{v}_r$ for round liquid jets correlated in the same manner as for plane liquid jets in terms of this streamwise variable. Finally, limits giving the onset of turbulent primary breakup along the surface, as well as the liquid column breakup length, are also shown in Fig. 9 to help define the region of the liquid surface where turbulent primary breakup can occur. These limits do not correlate in the same manner as ε and appear as bands rather than lines as a result.

There is a consistent tendency for values of ε to be somewhat smaller for round free turbulent jets than for nearly plane free turbulent jets in Fig. 9; however, the differences between the two sets of results are comparable to experimental uncertainties of the ε measurements. This suggests that the hydraulic diameter adequately represents the differences between the characteristic length scales Λ of round and plane turbulent freejets. The best-fit correlation of the combined measurements of ε for round and plane turbulent freejets, which is shown in Fig. 9, is as follows:

$$\varepsilon = 0.016\left[x \Big/ \left(\Lambda We_{f\Lambda}^{\frac{1}{2}}\right)\right] \tag{39}$$

The actual best-fit power of the independent variable of Eq. (21) is 0.97, with an experimental uncertainty (95% confidence) of 0.03, which is not statistically different from unity. Therefore, the simpler form used in Eq. (39) has been retained for the present data correlation. The standard deviations of the coefficient and power appearing on the right-hand side of Eq. (39) are 3 and 9%, respectively, and the correlation coefficient of the fit is 0.92, which is good. Moreover, the trends of the measurements illustrated in Fig. 9 appear to be quite reasonable. In particular, values of ε are relatively small, <0.01 near the onset of turbulent primary breakup, but approach

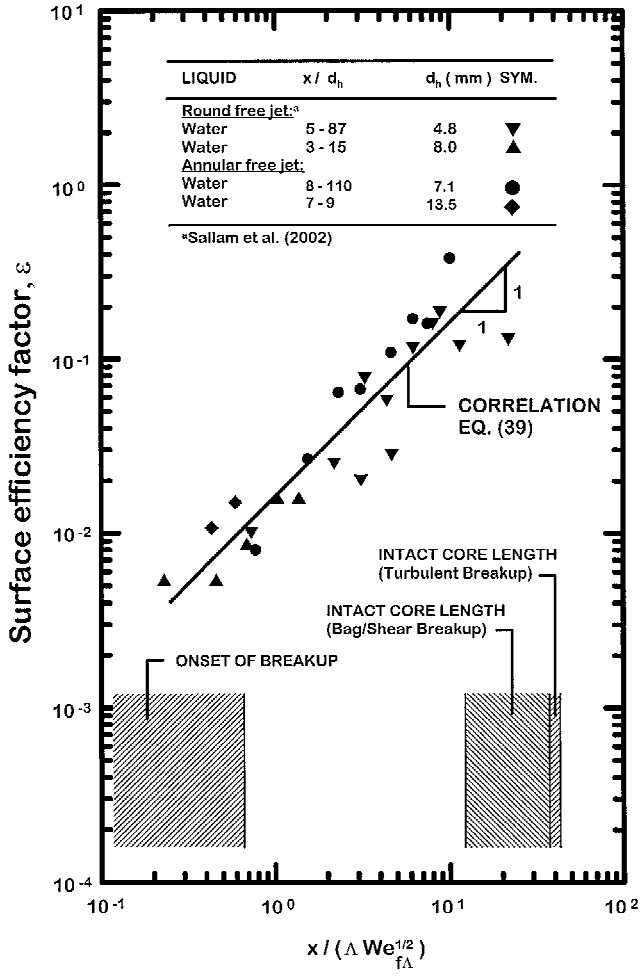

Fig. 9 Mean surface efficiency factors as functions of normalized streamwise distances for round and annular freejets in still air.

unity near the end of the liquid jet where the entire liquid column breaks up.

Conclusions

The formation of ligaments and drops during turbulent primary breakup along the surfaces of turbulent liquid jets in still air at NTP was studied experimentally. Test conditions involved round and annular (nearly plane) water and ethanol jets with fully developed turbulent pipe flow at the jet exit. Ranges of test variables were as follows: jet exit Reynolds numbers of 6×10^3–4.24×10^5, Weber numbers of 200–300,000, and liquid/gas density ratios of 690 and 860 at conditions where direct effects of liquid viscosity were small. The major conclusions of the study are as follows:

1) Ligament diameters at the onset of ligament formation could be explained by equating the surface tension energy required to form a ligament to the kinetic energy of the corresponding liquid eddy, relative to its surroundings within the inertial region of the turbulence spectrum.

2) Corresponding drop diameters at the onset of drop formation could be explained by the assumption that drops formed from the tips of the ligaments that first appeared at the onset of ligament formation due to Rayleigh breakup of these ligaments. This was the dominant mechanism of drop formation, generally observed more than 90% of the time. The alternative drop formation mechanism, observed less than 10% of the time, involved breakup of the entire ligament at its base due to velocity fluctuations in the liquid near its surface (at the base of the ligaments).

3) The location of the onset of ligament formation along the surface was associated with convection of eddies of appropriate size along the liquid surface for a time proportional to the characteristic times of these eddies. The location of the onset of drop formation, however, was associated with the Rayleigh breakup time of the drops formed at the onset of drop breakup because these times are significantly longer than the characteristic eddy times.

4) Ligament diameters progressively increase with increasing distance from the jet exit. This behavior could be associated with convection along the liquid surface for the progressively increasing Rayleigh breakup times that are required as ligament diameters increase. The corresponding increase of the SMD of drops after turbulent primary breakup with increasing distance from the jet exit then followed as a result of Rayleigh breakup of the progressively larger ligaments at each streamwise location as distance from the jet exit increased.

5) Mean streamwise drop velocities after turbulent primary breakup were essentially equal to mean streamwise velocities within the liquid jet, whereas mean relative cross stream drop velocities after turbulent primary breakup were proportional to rms cross stream fluctuating velocities in the liquid. An interesting feature about cross stream drop velocities near the jet exit is that they are actually larger than rms cross stream velocity fluctuations in fully developed turbulent pipe flow that is representative of liquid turbulence properties. (See Laufer's measurements of turbulence properties in fully developed turbulent pipe flow reported by Hinze.[28]) Thus, rather than being retarded by effects of surface tension that become small once turbulent primary breakup exceeds onset conditions, they are enhanced due to the reduced inertial resistance of a gas, as opposed to a liquid, beyond the liquid surface.

6) The mean drop mass flux $\dot{m}''_f$, due to turbulent primary breakup at the liquid surface, could be correlated with a surface efficiency factor defined as $\varepsilon = \dot{m}''_f/(\rho_f \tilde{v}_r)$, in terms of the streamwise variable $x/(\Lambda We_{f\Lambda}^{1/2})$, which also controlled variations of ligament diameter, drop SMD after turbulent primary breakup, and cross stream relative drop velocities after turbulent primary breakup along the liquid surface. Quite plausibly, ε was small near the onset of drop formation due to turbulent primary breakup, but reached values on the order of unity as the end of the liquid core of the jet is approached.

7) Effects of geometry changes from round to annular (nearly plane) turbulent liquid jets influence the radial integral scale Λ that is used to normalize distance scales for turbulent primary breakup properties. The present results, however, showed that these effects could be handled adequately with the hydraulic diameter of the turbulent jet, given that $\Lambda = d_h/8$ based on Laufer's measurements of fully developed turbulent pipe flows (see Ref. 28).

Acknowledgments

This investigation was sponsored by the U.S. Office of Naval Research, Grant N00014-95-1-0234, under the technical management of E. P. Rood. Initial development of research facilities for the investigation was carried out under U.S. Air Force Office of Scientific Research Grant AFOSR 49620-95-1-0364 under the technical management of J. M. Tishkoff.

References

[1]De Juhasz, K. J., Zahn, O. F., Jr., and Schweitzer, P. H., "On the Formation and Dispersion of Oil Sprays," Engineering Experiment Station, Bulletin 40, Pennsylvania State Univ., University Park, PA, 1932.

[2]Lee, D. W., and Spencer, R. C., "Preliminary Photomicrographic Studies of Fuel Sprays," NACA TN 424, 1933.

[3]Lee, D. W., and Spencer, R. C., "Photomicrographic Studies of Fuel Sprays," NACA TN 454, 1933.

[4]Schweitzer, P. H., "Mechanism of Disintegration of Liquid Jets," *Journal of Applied Physics*, Vol. 8, 1937, pp. 513–521.

[5]Grant, R. P., and Middleman, S., "Newtonian Jet Stability," *AIChE*, Vol. 12, 1966, pp. 669–678.

[6]Phinney, R. E., "The Breakup of a Turbulent Jet in a Gaseous Atmosphere," *Journal of Fluid Mechanics*, Vol. 60, 1973, pp. 689–701.

[7]McCarthy, M. J., and Malloy, J. J., "Review of Stability of Liquid Jets and the Influence of Nozzle Design," *Chemical Engineering Journal*, Vol. 7, 1974, pp. 1–20.

[8]Hoyt, J. W., and Taylor, J. J., "Turbulence Structure in a Water Jet Discharging in Air," *Physics of Fluids*, Vol. 20, Pt. 2, 1977, pp. S253–S257.

[9]Hoyt, J. W., and Taylor, J. J., "Waves on Water Jets," *Journal of Fluid Mechanics*, Vol. 83, 1977, pp. 119–127.

[10]Ruff, G. A., Sagar, A. D., and Faeth, G. M., "Structure and Mixing Properties of Pressure-Atomized Sprays," *AIAA Journal*, Vol. 27, No. 7, 1989, pp. 901–908.

[11]Ruff, G. A., Bernal, L. P., and Faeth, G. M., "Structure of the Near-Injector Region of Pressure-Atomized Sprays," *Journal of Propulsion and Power*, Vol. 7, No. 2, 1991, pp. 221–230.

[12]Ruff, G. A., Wu, P.-K., Bernal, L. P., and Faeth, G. M., "Continuous- and Dispersed-Phase Structure of Dense Nonevaporating Pressure-Atomized Sprays," *Journal of Propulsion and Power*, Vol. 8, No. 2, 1992, pp. 280–289.

[13]Tseng, L.-K., Ruff, G. A., and Faeth, G. M., "Effects of Gas Density on the Structure of Liquid Jets in Still Gases," *AIAA Journal*, Vol. 30, No. 6, 1992, pp. 1537–1544.

[14]Wu, P.-K., Tseng, L.-K., and Faeth, G. M., "Primary Breakup in Gas/Liquid Mixing Layers for Turbulent Liquids," *Atomization and Sprays*, Vol. 2, No. 3, 1992, pp. 295–317.

[15]Wu, P.-K., and Faeth, G. M., "Aerodynamic Effects on Primary Breakup of Turbulent Liquids," *Atomization and Sprays*, Vol. 3, No. 3, 1993, pp. 265–289.

[16]Wu, P.-K., Miranda, R. F., and Faeth, G. M., "Effects of Initial Flow Conditions on Primary Breakup of Nonturbulent and Turbulent Round Liquid Jets," *Atomization and Sprays*, Vol. 5, No. 2, 1995, pp. 175–196.

[17]Wu, P.-K., and Faeth, G. M., "Onset and End of Drop Formation Along the Surface of Turbulent Liquid Jets in Still Gases," *Physics of Fluids A*, Vol. 7, No. 11, 1995, pp. 2915–2917.

[18]Sallam, K. A., Dai, Z., and Faeth, G. M., "Liquid Breakup at the Surface of Turbulent Round Liquid Jets in Still Gases," *International Journal of Multiphase Flow*, Vol. 28, 2002, pp. 427–449.

[19]Dai, Z., Hsiang, L.-P., and Faeth, G. M., "Spray Formation at the Free Surface of Turbulent Bow Sheets," *Proceedings of the Twenty-First Symposium on Naval Hydrodynamics*, National Academy Press, Washington, DC, 1997, pp. 490–505.

[20]Dai, Z., Chou, W.-H., and Faeth, G. M., "Drop Formation Due to Turbulent Primary Breakup at the Free Surface of Plane Liquid Wall Jets," *Physics of Fluids*, Vol. 10, No. 5, 1998, pp. 1147–1157.

[21]Sallam, K. A., Dai, Z., and Faeth, G. M., "Drop Formation at the Surface of Plane Turbulent Liquid Jets in Still Gases," *International Journal of Multiphase Flow*, Vol. 25, No. 6–7, 1999, pp. 1161–1180.

[22]Simmons, H. C., "The Correlation of Drop-Size Distributions in Fuel Nozzle Sprays," *Journal of Engineering for Power*, Vol. 99, No. 3, 1977, pp. 309–319.

[23]Merrill, C. F., and Sarpkaya, T., "Spray Formation at the Free Surface of a Liquid Wall Jets," AIAA Paper 98-0442, Jan. 1998.

[24]Tyler, E., "Instability of Liquid Jets," *Philosophical Magazine*, Vol. 16, 1933, pp. 504–518.

[25]Weber, C., "Zum Zerfall eines Flussigkeitsstrahles," *Zeitschrift Angewesen Mathematica Mechanic*, Vol. 2, 1931, pp. 136–141.

[26]Mazallon, J., Dai, Z., and Faeth, G. M., "Primary Breakup of Nonturbulent Round Liquid Jets in Gas Crossflows," *Atomization and Sprays*, Vol. 9, No. 3, 1999, pp. 291–311.

[27]Tennekes, H., and Lumley, J. L., *A First Course in Turbulence*, MIT Press, Cambridge, MA, 1972, pp. 248–296.

[28]Hinze, J. O., *Turbulence*, 2nd ed., McGraw–Hill, New York, 1975, pp. 427 and 724–734.

S. K. Aggarwal
Associate Editor